



Optimizing Machine Tool Assembly Stiffness Using CAE-Based Analysis and Simulation

Ravi Kumar L¹, Nagesh N², K Ganesh³

¹Assoc. Professor & HOD, Department of Civil Engineering, Kuppam Engineering College, Kuppam-517425

²Assoc. Professor, Department of Mechanical Engineering, Kuppam Engineering College, Kuppam-517425

³Assoc. Professor & HOD, Department of Mechanical Engineering, Kuppam Engineering College, Kuppam-517425

Abstract: Machine tool manufacturers are working hard to keep their competitive advantage in the current unstable economy and global marketing environment by creating creative designs that meet the demands of modern production, such as high precision, accuracy, and dependability. Therefore, the construction of machine tool structures is crucial since they have a direct impact on the factors that determine a machine's capability, motion accuracy, productivity, and machining quality. By building the structure with the ideal amount of static and dynamic stiffness, this can be accomplished. Nowadays, when developing machine structural components, the goal is to minimize the weight of the machine structure while maintaining the appropriate threshold values for both static and dynamic mechanical qualities. Finite Element Analysis is a technique used to do this.

In the present study structural analysis of the Double Column Vertical Machining Centre is carried out using Cosmo works software. The analysis involves static deformations and strain in structure that is bearing the static forces and design solutions are proposed to optimize the machine structure with maximum deformation in order to have optimum static stiffness, so that balance between productivity and accuracy is achieved. Stiffness of the machine structure for static loads is evaluated by modelling the columns, cross-beam, and cross-slide and ram assembly. Percentage contribution of all the structural members towards the overall deflection at the tool tip is determined. Ram is found to be the important member contributing to the overall deflection at tool tip.

Hence detailed analysis of the ram carried out. Various design alternatives are studied to optimize the ram with the objective of increasing its stiffness with minimum weight addition or maintaining same weight w.r.t existing ram and decreasing the tool point deflection which in turn increases the stiffness of machine.

Keywords: VMC, steel, Ductile cast-iron, Cosmos, software and optimization

I. Introduction:

The majority of early research work in the field of machine tool structures was directed towards obtaining the data concerning the static and dynamic characteristics of machine tool structural elements like base ram, column etc. The majority of these early studies were experimental and FEA based studies in the improvement of the machine tool structure stiffness. Y. Atlantis, C. Brecher, M. Weck, S. Witt described current state of Virtual Machine Tool Technology and related on-going research challenges. The structural analysis of machine tools using Finite Element models and their experimental calibration techniques are presented. The kinematic analysis and optimization of machine tool elements are discussed with sample examples. The interaction between the control of the feed drives, cutting conditions and machine tool structure is presented. Multi-body dynamic models of the machine, which allow integrated simulation of machine kinematics, structural dynamics and control techniques, are discussed. The interaction between the machine tool, controller and cutting process disturbances are discussed with sample examples. The simulation of machining operation and its impact on the dynamics of the machine tool and CNC are elaborated. The paper presents both the summary of current and past research, as well as research challenges in order to realize a fully digitized model of the machine tool. [1] D. Spath, W. Neithardt, C. Bangert conducted an investigation on the structural optimization of micro milling machine. The 3-axis micro-milling machine is used for study the machine frame basically consists of welded machine base and column with several internal ribs is analysed for high and dynamic stiffness. The machine column is found to be less stiffer. Its optimized structure, which consists of two large outer ribs converging towards the top and thickening at the edges. A. Cowley and S. Hinduja described the development of the program for computation of the static deformation of machine tool structures and structural elements. The program was based upon the finite element technique and the structure was subdivided into rectangular and triangular plates like elements and the beam like elements. Special attention was given to consideration of the basic deformation shapes of the individual elements and their influence upon the accuracy of the resulting deformation of the overall structure. The accuracy of the program was evaluated by its application to simple plate and box structure to various loading conditions and the results obtained by finite element based beam model were compared with experimentally measured values for knee type-milling machine.



From the comparison, it was stated that beam model results agreed quietly well with experimentally measured values. However in FEA model the machine was assumed to be rigidly fixed at the base, where as some flexibility would be apparent at the bolted flange in real life situation. A. C. Stephen and S. Taylor discussed the advantages of analytical techniques like flexibility method and stiffness method compared to finite element technique for structural analysis of machine tool. It was stated that in finite element technique the displacement method was used exclusively because the idealization of structures into assemblies of plate and beam elements invariably results in high degree of redundancy. Beam elements, triangular and rectangular plate elements present in the panels. It was suggested to use many nodes in the regions of high stress gradients and avoid the use of long narrow elements. The finite element method was presented and shown to be valuable addition to analytical techniques available to machine tool structural designers.

II. Material and Methods:

1. Steel (IS 5120)

A metal consisting of iron and up to approximately 1.5% carbon, usually with small amounts of manganese, phosphorus, sulphur, and silicon as well.

Table 4.1 Material Composition of steel

C%	Mn%	P%	S%	Si%	Cr%
0.17-0.22	0.70-0.90	0.035(max)	0.04	0.15-0.30	0.70-0.90

2. Gray cast iron

A type of cast iron with high levels of carbon and excellent compression strength. Gray cast iron is the most common cast iron.

Table 4.2 Material Compositions of a gray cast iron

C%	Si% + Mn%+S%
1.5-4.5	0.3-5

3. Ductile cast iron

A type of cast iron with a similar composition to gray cast iron, but with improved ductility. Ductile cast iron contains tiny spheres of graphite. SG iron is called as spheroidal graphite cast iron, or also called as ductile cast iron

Table 4.3 Material Composition of a ductile cast iron

C%	Si%	Mn%	S%	P%	Cr%
2.7-3.8	0.5-3.8	0.2-0.7	≤0.02	≤0.1	≤0.15

Table 4.4 the mechanical properties of commonly used materials in machine tool

PROPERTIES / MATERIAL	STEEL(IS5120)	GRAY CASTIRON	DOCTILE CASTIRON
Young's modulus	2.1×10^5 Mpa	$0.8 - 1.48 \times 10^5$ Mpa	$1.6 - 1.8 \times 10^5$ Mpa
Density	7850×10^{-9} Kg/mm ³	$7100 - 7400 \times 10^{-9}$ Kg/mm ³	$7100 - 7400 \times 10^{-9}$ Kg/mm ³
Damping ratio	0.0001	0.001	0.002-0.003
Thermal exp. Coeff.	11×10^{-6} k	$11 - 12 \times 10^{-6}$ k	$11 - 12 \times 10^{-6}$ k

III. Analysis of DMC2000N

1. Importing CAD model and applying materials.

The CAD model Ram, Cross-Slide, Cross-Beam, Column-left and Column-right with ball screws and LM-guide ways are modelled and each part is mated to form the assembly of the machine structure in the solid works. The mated assembly is imported to simulation work bench called Cosmos works. Cosmos works is a design analysis system fully integrated with Solid Works. Cosmos works supports IGES and all formats of solid- works. The software provides easy transfer of model to FEA workbench avoiding all tedious, time-wasting tasks associated with creating and analysing the virtual prototype by CAE engineers, these include CAD geometry translation, geometry clean-up, manual meshing processes, assembly connection definition, and editing of input decks to setup jobs for analysis by various solvers .After importing the model into the simulation work bench, the each part are assigned material by which are to be manufactured such as ,Ram-SG1 cross-slide, crossbeam and columns-G4.The properties of materials used are detailed in table7.1.

The fig 7.1 shows the material assignment for all the parts which is considered for analysis.

Table 7.1 Properties of the materials used for machine components

PROPERTIES	G4 (GREY CAST IRON)	SG1 (DUCTILE CAST IRON)	HARD STEEL (Is-5120)
Young's modulus Mpa	1.35×10^5	1.74×10^5	2.9×10^5
Density Kg/mm ³	7500×10^{-9}	7350×10^{-9}	5200×10^{-9}
Poisson ratio	0.26	0.29	0.3
Shear modulus Mpa	5.6×10^4	8.3×10^4	8.5×10^4
Tensile strength Mpa	3×10^2	5.86×10^2	7.38×10^2
Compressive strength Mpa	9.6×10^2	8.79×10^2	9.38×10^2
Modules	Column (LH&RH), Cross slide, Cross beam	Ram	Ball screw, LM guide ways

2. Setting up the boundary conditions

Forces apply along with the x, y, and z direction.

Displacement : All DOF

Pressure / Force : self weight (mass of the component) and cutting force (736.6kgf)

2.1. Constraining the model

The cross beam is located on the column to form a bridge. The interaction between columns and the cross beam is achieved by applying spider bolt model at the locations of the bolt holes shown in fig 7.3.

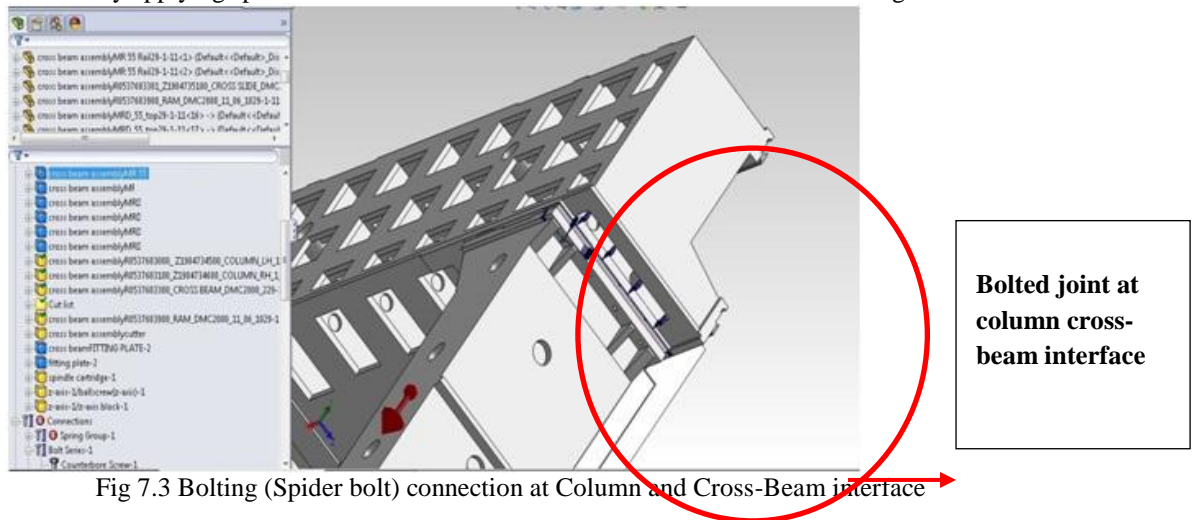


Fig 7.3 Bolting (Spider bolt) connection at Column and Cross-Beam interface

The column is clamped on to the base to simulate it the x and z-axes translational movements are constrained at the clamping area of the column. The location of the constraint is shown in fig7.4.

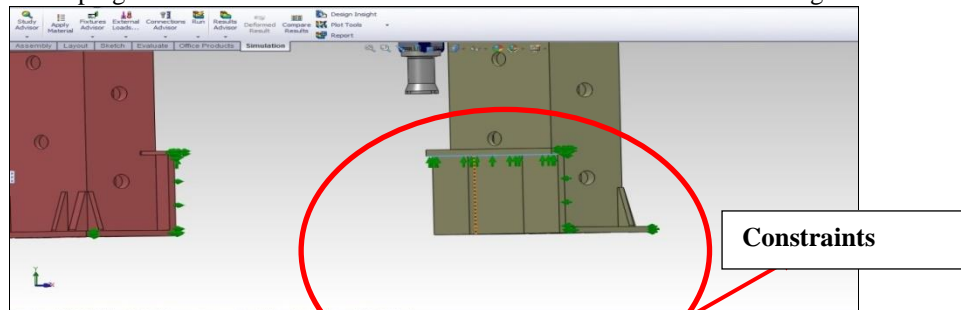


Fig 7.4 Column Bottom View showing the FE constraints

2.3 Applying loads

The study confined to static study in machine tool the static loads acting on the structure are self-weight (mass of component), cutting forces. The cutting forces are generated at tool tip due to cutting process. The cutting force of 736.3Kgf is applied to tool tip in X, Y and Z-directions for computation.

The fig 7.5 shows detailed view of loads applied and constraints applied for the FEA model of structural assembly.

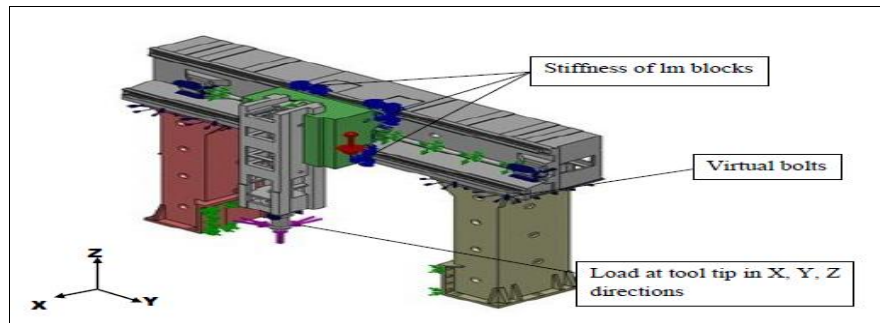


Fig 7.5 FEA constraints applied to Structural Assembly.

2.4 Meshing and Solving

Meshing is the process of Discretization of the model in finite elements to facilitate analysis. Meshing here done using semiautomatic mesh. The results of the FEA models are dependent on the mesh element size optimum mesh size for assembly model is done. The tools are provided to check the mesh quality such as Jacobian checks, aspect ratio check. The details of meshing are given in table 7.5. The fig 7.6 shows the assembly with detailed mesh.

Table 7.5 Meshing information Details

Total Nodes	374959
Total Elements	197760
Maximum Aspect Ratio	38.307
% of elements with Aspect Ratio < 3	77.4
% of elements with Aspect Ratio > 10	0.599
% of distorted elements(Jacobian)	0
Time to complete mesh(hh:mm:ss)	00:02:09
Computer name:	CPE4100408

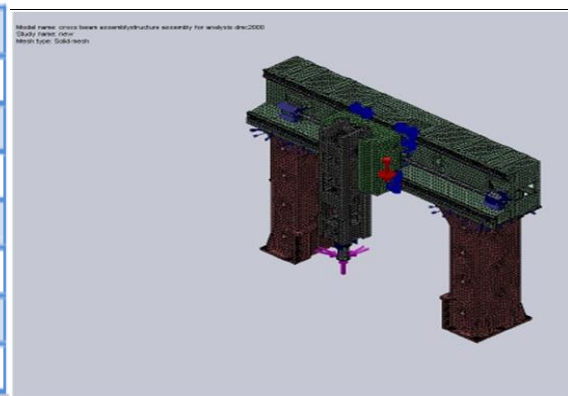


Fig 7.6 Detailed Meshed Model

2.5 Analysis

After applying the boundary condition the solution of the model under study is carried out in Cosmo works. The displacement along X,Y,Z-direction and resultant, stress are studied

- Displacement - resultant.
- Displacement along X-direction.
- Displacement along Y-direction.
- Displacement along Z-direction.
- Stress plot

The results of the stress plots and deflection plots are shown in fig 7.7 to 7.11

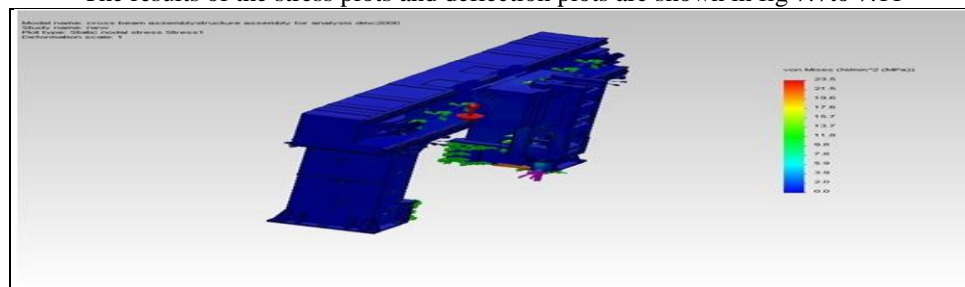
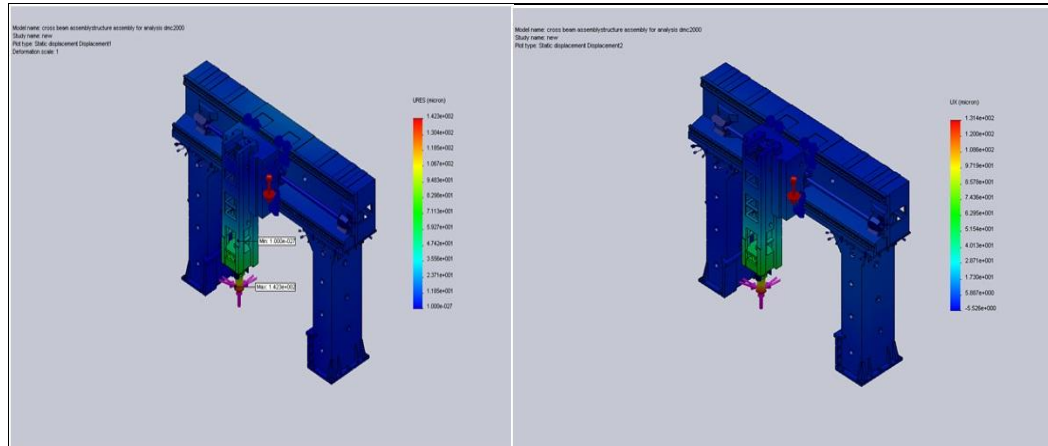


Fig 7.7 shows the stress plot for the applied load in X, Y, Z-directions



It is evident from the fig 7.9 that the max stress acting on the machine structure assembly is 23Mpa for applied load 736.3Kgf in each direction. The allowable stress is 64Mpa for G4 where as for SG iron it is 98Mpa [cmti].thus the stress in assembly well below the allowable stress and design is safe from strength consideration.



Shows the Resultant Displacement Plot

Shows the Deflection in X-direction.

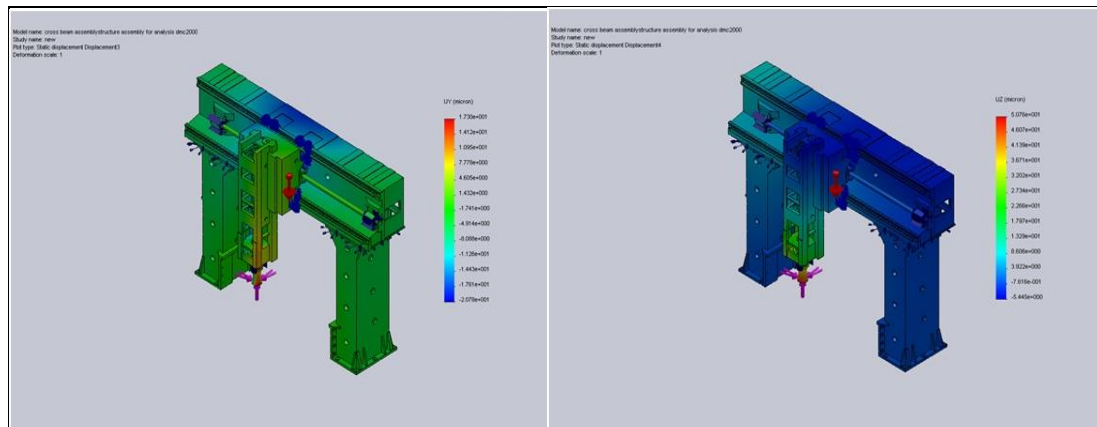
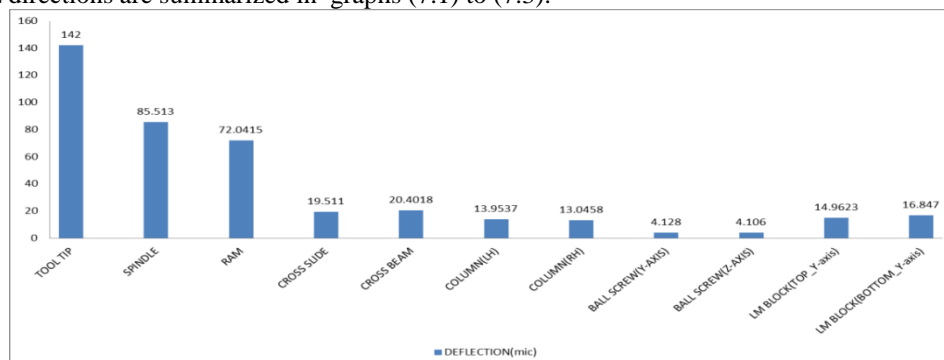


Fig 7.10 Shows the Deflection in Y-direction.

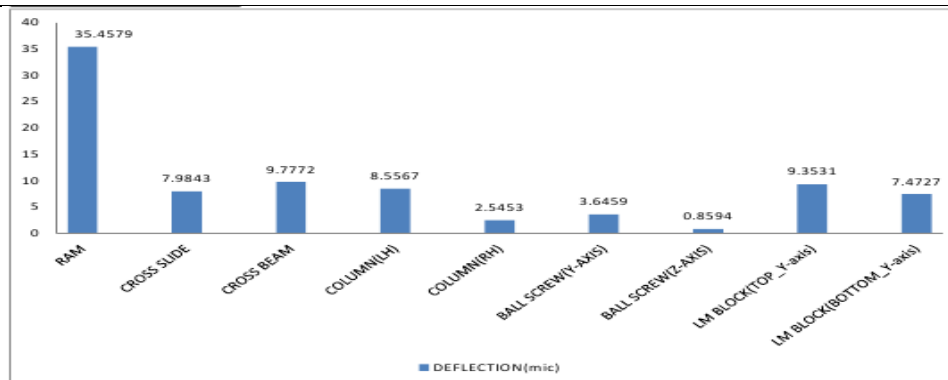
Fig 7.11 Shows the Deflection in z-direction

7.2.6 Interpretation of the results

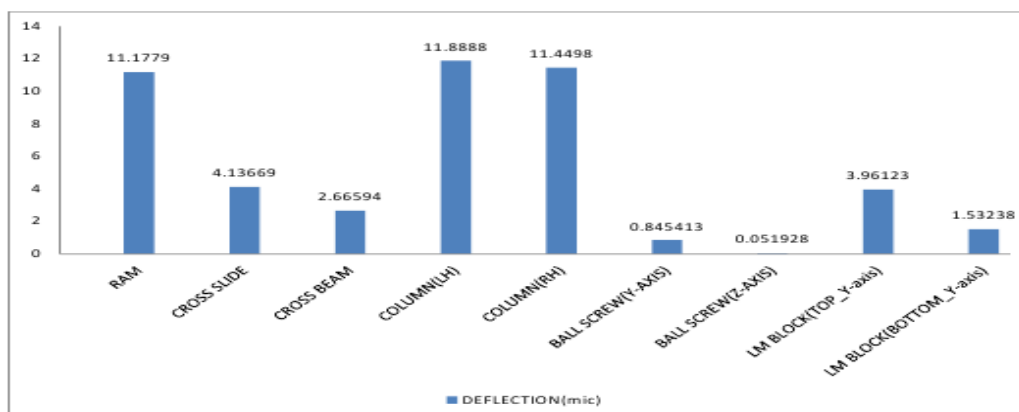
From analysis above further the deflection of each component for resultant and along each directions i.e. X, Y and Z directions are summarized in graphs (7.1) to (7.3).



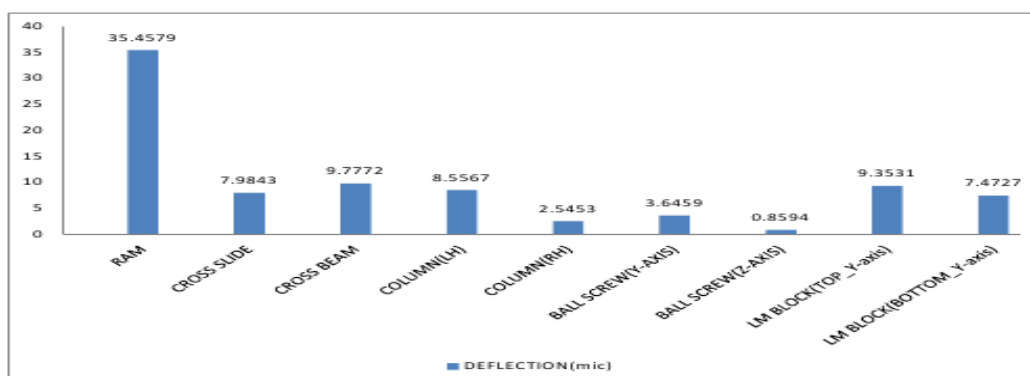
Graph 7.1 shows resultant deflection of each component



Graph 7.2 Shows Deflection of each component in X-direction



Graph 7.3 shows Deflection of each component in Y-direction



Graph 7.4 shows Deflection of each component in Z-direction

It is evident from the graphs shown above that the ram is deflected maximum among all the other components thus it is concluded that Ram is the important and weaker part and is taken up for further analysis.

IV. Analysis and Optimization of Ram

The ram is taken up for further analysis in order to maintain the constraints of the system the ram changes are made and the analysis is done in the assembly state only the mass of the existing ram is 997.6. It observed in the above results that the deflection in max at the bottom portion of the ram ie.675mm from the spindle mounting end. Hence the corrective measure to improve the stiffness of the part is done in iterative process. The deflection of the existing ram is shown in the table

Table 7.6 The deflection of the existing ram

Resultant in microns	X in microns	Y in microns	Z in microns
72.015	63.45	11.18	35.45

Once the exact deflection at the tool point is due to ram is known, the alternative are analysed for achieving optimum reduction in deflection of the ram which in turn decreases the defection at tool tip. The goal is to obtain high stiffness. The following are design alternatives studied in this regard.

Case1: Ram is analysed for the increase of wall thickness of the ram for a length of 675mm from the bottom in the increments of 10mm the fig 7.12 shows the c/s view of the ram showing the walls whose thickness is modified. The graph shows the decrease in deflection with increase of thickness. in this iteration it is observed that with increase in thickness for every 10mm the weight increased by 30kg and deflection reduced by 10 μ finally for 40mm (max thickness that can be increased) the deflection decreased to 110 μ .the deflection. The weight increased is more compared to deflection thus cannot considered. The fig7.13 shows the sensor results of ram for the change of 40mm wall thickness increase.

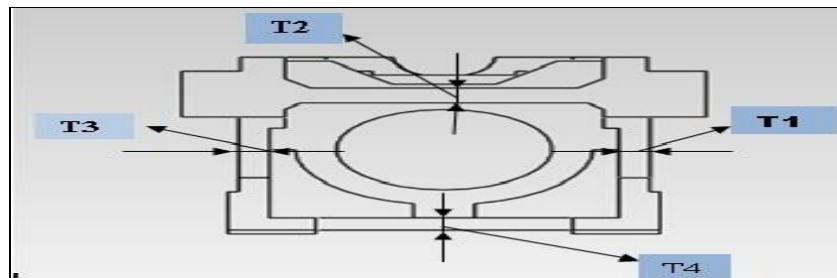
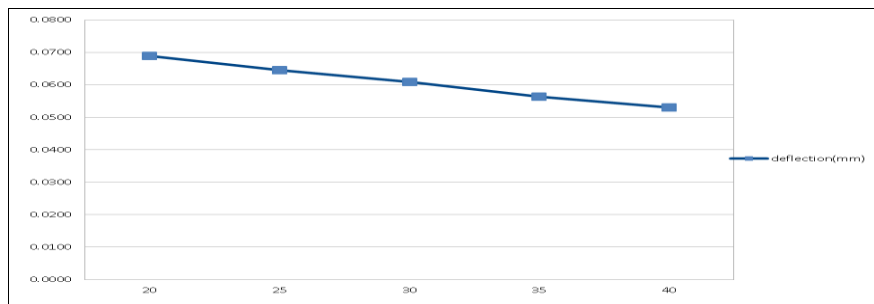


Fig7.12 C/S view of the Ram



Graph7.5 shows the change in deflection for increase in wall thickness (t_1, t_2, t_3, t_4). (Up to 650mm of ram from bottom).

Table 7.7 comparison of deflection values of case1 (for 40mm thk wall)

	Before iteration	After iteration
Deflection(in microns)	$U_{Res}-72.015, U_X-63.45,$ $U_Y-11.18, U_Z-35.45$	$U_{Res}-59.29, U_X-52.49,$ $U_Y-7.4, U_Z-27.487$
Weight(kg)	997.67	1250

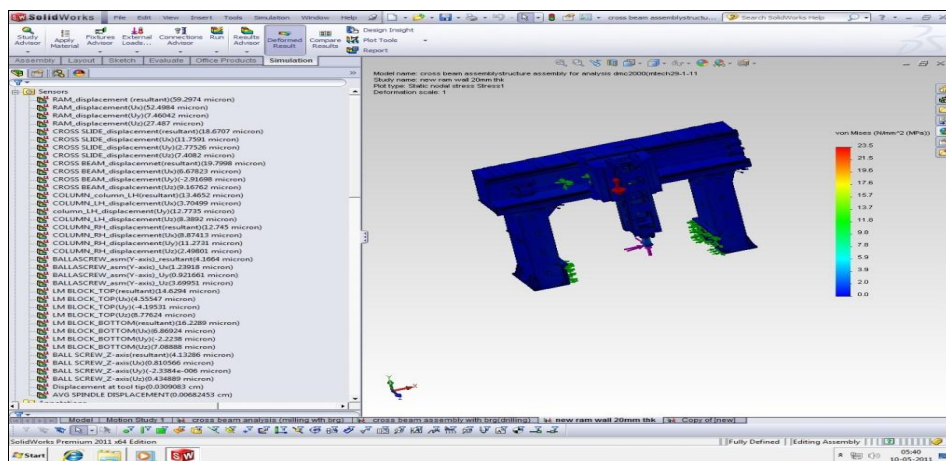


Fig 7.13 shows sensor results for 40mm increase in wall thickness.



Case 2: In this case the ram side walls are closed which are used for service using cover plate (well fit plate).the plate is fitted to ram using bolts. The resultant deflection is decreased by 14 microns (72μ to 58μ) and weight increased by only 3%(997.67kg to 1028kg).the tool point deflection reduced from 142μ to 105μ .The fig 7.14 shows the sensor reports of the ram and tool point deflection.

Table7.8 Comparison of deflection values of case2

	Before iteration	After iteration
Deflection(in microns)	$U_{Res}-72.015, U_X-63.45,$ $U_Y-11.18, U_Z-35.45$	$U_{res}-59.29, U_X-52.49, U_Y-7.4,$ $U_Z-27.487$
Weight(kg)	997.67	1028

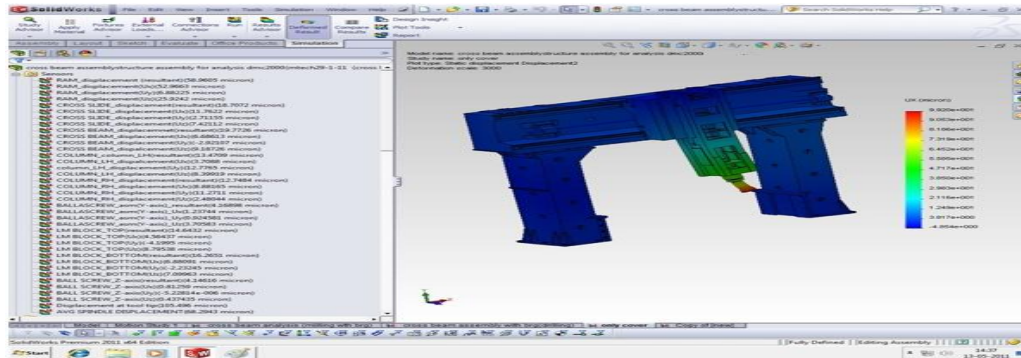


Fig 7.14 Showing The Existing Ram and Ram of case2

Case3: In this case the ram side opening and front opening both are closed which are used for service using cover plate (well fit plate).The plate is fitted to ram using bolts. The resultant deflection of the Ram is decreased by 20 microns (72μ to 52μ) and weight increased by only 3.25 %(997.67kg to 1050kg).The tool point deflection reduced from 142μ to 100μ which is the required deflection tolerance as per the user defined data. The fig 7.15shows the sensor reports of the ram and tool point deflection. The torque of the bolts to be 440N-m calculated using formula.

Table 7.9 Comparison of deflection values of case3

	Before iteration	After iteration
Deflection(in microns)	$U_{Res}-72.015, U_X-63.45,$ $U_Y-11.18, U_Z-35.45$	$U_{res}-52.10, U_X-48.118,$ $U_Y-6.88, U_Z-22.46$
Weight(kg)	997.67	1050

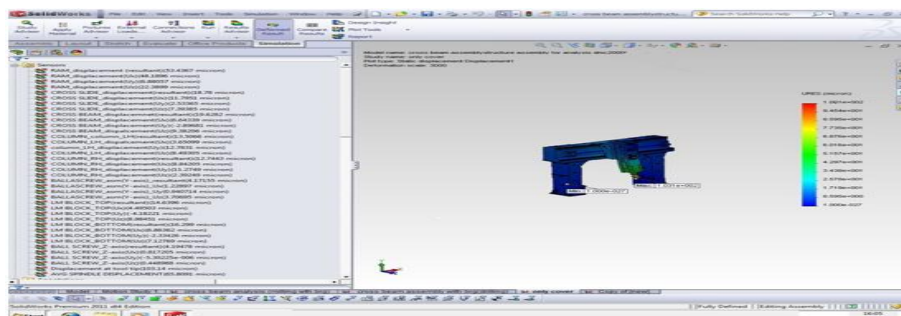


Fig 7.15 Showing The Existing Ram and Ram of case3

Case 4: In this case the ram material have been changed from SG1 to S1(Cast carbon steel).The selection of material is based on the young's modulus since the deflection is inversely proportional to young's modules refer eqn 7.1 .the properties of material is tabulated in table 7.10. The resultant deflection of the Ram is decreased by 14 microns (72μ to 57μ) and weight increased by only 11 %(997.67kg to 1124kg).The tool point deflection reduced from 142μ to 102μ which is the required deflection tolerance as per the user defined data. But the mass of the component is more compared case 3 and deflections are less in case3. At the same time cost of steel is more than SG1 so this case is eliminated.fig7.16 shows the sensor results of ram and tool tip deflection.



$$\delta = \frac{PL}{AE} \dots \dots \dots \text{Eqn7.1}$$

Where, δ =deflection, P=applied load, L=length, A=c/s sectional area.

Table 7.10 shows the properties of existing and new material

Properties	Units	SG1	S1
Young's modulus	N/mm ²	1.74×10^5	2.1×10^5
Mass density	Kg/mm ³	7350×10^{-9}	7800×10^{-9}
Poisons ratio		0.29	0.3
Shear modulus	N/mm ²	8.34×10^4	8.5×10^4
Tensile strength	N/mm ²	5.86×10^2	7.38×10^2
Compressive strength	N/mm ²	8.79×10^2	9.4×10^2
Module	Ram	Existing material	New material

Table 7.11 Comparison of deflection values of case4

	Before iteration	After iteration
Deflection(in microns)	U _{Res} -72.015, U _X -63.45, U _Y -11.18, U _Z -35.45	U _{res} -57.10, U _x -51.28, U _y -6.12, U _z -22.46
Weight(kg)	997.67	1124

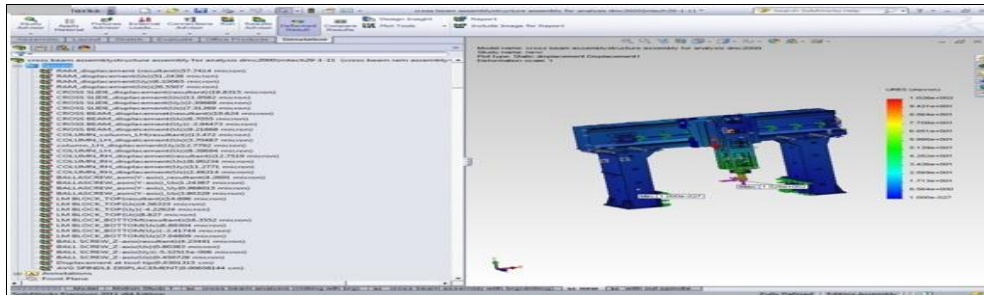


Fig 7.16 shows the sensor results of Ram for Case 4.

7.4 Summary

Among the iterations made the case 3 iteration is considered to be the best that is the cover plate design for both the openings at the bottom. Though the case 4 is also suitable but the cost of material is high and casting of steel is also difficult. Hence case3 is preferred over the case 4.

The comparison of tool tip deflection results with existing and case 3 is shown in fig 7.17. It is evident that the ram with closed opening has decreased the tool tip deflection thus the stiffness at the tool tip is increased from 51N/μ-m to 72 N/μ-m which in turn improves the accuracy and also productivity of the machine.

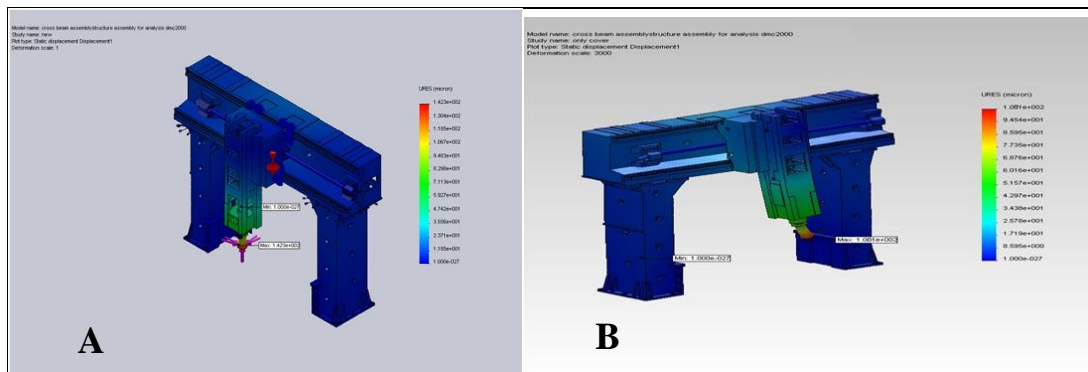


Fig 7.17 shows (A) Existing tool deflection (B) tool deflection for case 3

V. Results and Discussions

In the present work an attempt has been made to find the stiffness of the double column vertical machining centre, the deflection contribution of its structure to the total deflection at the tool tip and redesign of the Ram to have higher stiffness and tool point deflection to be within the users requirement with minimal



increase of weight under the static condition. CAE technique (FEA) is used for the purpose. The stiffness of the machining centre assembly like ram, cross-slide, cross-beam, column-LH, column-RH to the total deflection at tool point is found from the static analysis of the assembly structure. Stiffness evaluation indicated that ram is the weaker member. Subsequently, detailed analysis of the Ram is carried out and various design alternatives are suggested as discussed in chapter 7. The change in deflection and weight during the different iterations are given in the Table 8.1.

Table 8.1 Changes in deflection and weight for different iteration.

Iterations	Change in deflection in Ram	Change in deflection at tool point	Change in Weight
Case1	13 μ decrease	20 μ decrease	9% increase
Case2	14 μ decrease	35 μ decrease	3% increase
Case 3	20 μ decrease	Decreased by 42 μ (142 to 100)	5% increase
Case4	14 μ decrease	Decreased by 40 μ (142 to 102)	11% increase

VI. Conclusion

The structural analysis of the DMC2000N is carried out using cosmoworks2011. Five modules viz., Ram, Cross-slide, Cross-beam, Column-LH, Column-RH are considered for analysing the stiffness by applying FEA. The following conclusion could be drawn.

1. The load is applied at the tool tip and the work-piece is transmitted as internal forces through the structure onto the nodes within the interfacial areas, which are between two connecting modules. There is no need to transform the external loading into equivalent forces to be applied at the interfacial areas on the single module. Possible human errors occurring during transformation of loading is reduced to a greater extent.

2. Stiffness of the machine centre and contribution of its members to total deflection is evaluated from the results of the analyses, which showed that the Ram is the weakest part among the modules. Subsequently Ram is taken up for optimization with respect to increase in rigidity.

3. The ram is redesigned by changing the wall thickness, cover plate design for the opening on the walls of Ram and change of material. Finally the cover plate design alternative is chosen as best alternative.

4. The Ram stiffness is optimized with optimal addition of material compared to existing one by adapting the method of using cover plates (well-fit plates). The Ram deflection is reduced by 20 microns with the reduction of deflection at tool point from 142 microns to 100 microns. Now the Ram stiffness has been increased by 20 N/ μ m.

The primary contribution of the project is to introduce an alternative method for obtaining stiffness of machine tool. The method is highly advantageous in obtaining stiffness of complex machines and assemblies easily and efficiently with higher accuracy than traditional method. The ram is found to be weakest of all modules in X and Z directions. The ram optimization is made possible with optimal utilization of material and also the stiffness of tool is increased which increases the accuracy, productivity of machine.

VII. Reference

- [1]. Y. Atlantis, C. Brecher, M. Weck, S. Witt, Virtual machine tool technology, proc 25th MTDR, 2008.
- [2]. D. Spath, W. Neithardt, C. Bangert, the structural optimization of micro milling machine, Machines and Mechanism, 1999.
- [3]. A. Cowley and S. Hinduja, Finite Element method for analysis of machine tool structures, proc 10th conf 1969.
- [4]. A. C. Stephen and S. Taylor, Computer analysis of machine tool structure by Finite Element Method. proc 5th Machine Tool Design and research conference 1965.
- [5]. Masamitsu Nakminami, Tsutomu Tokuma, Kazuhiko Matsumoto and Keiichi Nakamoto, the design methodology for compound multiaxis machine tools, proc 15th, machine tool design and research conference 1999.
- [6]. H. Weule, J. Fleischer, W. Neithardt, D. Emmrich and D. Just, FEA analysis of machine tool structure and the use of topology optimization., Machines and Mechanism, 2001.
- [7]. S. Haranath, N. Ganesan and B. V. Rao, Dynamic Analysis of machine tool structure with applied damping treatment, Int J. Mach. Tools Manufacture. Vol. 27, No 1, p. 43-55, 1987.
- [8]. P. De Fonseca*, D. Vandepitte, H. Van Brussel, P. Sas., Dynamic analysis of machine tool in workspace., Int J. Mach. Tools Manufacture. Vol. 42, No 1, p. 43-55, 2003.
- [9]. J. N. Dube, Computer aided design of milling machine structure, proc 7th A.I.M.T.D.R Conf 1965.
- [10]. R.C. Bahl and P.C. Pandey investigations into Deformation Behaviour of ribbed machine tool Column, Proc. of AIMTDR 1978.
- [11]. Koenigsbeger, F., Design principles of metal Cutting machine Tools. vol 1 Pergamon press 1970.



- [12]. Manfred Weck Handbook of Machine Tools.Vol 1-4.
- [13]. M.K. Mehtha, Machine Tool Design ,Tata McGraw Hill1984
- [14]. Singiresu. S. Rao The Finite Element Method in Engineering, springer,2006
- [15]. Sen and Bhatta Charaya Principle of Machine Tools, New Cetral Book, reprint. 1995
- [16]. BFW Material Standard Manual